Pseudorandom Noise Sequence Time-Modulated Reflective Metasurfaces for Target Recognition

Xiaoyi Wang, *Member, IEEE*, Mei Song Tong, *Senior Member, IEEE*, and Lei Zhao, *Senior Member, IEEE*

***Abstract*— In this article, pseudorandom noise (PN) sequence time-modulated reflective metasurfaces are proposed to provide a low-cost, low-complexity, simple solution for target recognition. By covering the target to be recognized with a time-modulated metasurface modulated by a PN time sequence, the metasurface scatters the interrogating harmonic wave into a binary PN-modulated wave. As a result, the radar detector with the foreknowledge of the modulating PN sequence may recognize the target by applying the properties of strong autocorrelation and weak cross correlation of PN sequences and performing cross correlation between the modulating PN sequence and the picked-up signal after downshifting its frequency without actually decoding and reading the scattered information. A 1-bit reconfigurable metasurface unit cell operating at 2.4 GHz is proposed and full-wave simulated to achieve out-of-phase reflective responses by controlling the ON and OFF states of the p-i-n diode for PN time modulation. The target recognition is demonstrated by experiment in two different scenarios where only one metasurface and multiple metasurfaces are present for recognition. The experimental results show that by providing an appropriate threshold in the cross-correlation detecting results, the proposed method can recognize the targets well in both scenarios.**

***Index Terms*— Autocorrelation, cross correlation, Dirac delta function, pseudorandom noise (PN) sequence, radars, target recognition, time-modulated metasurfaces.**

I. Introduction

TARGET recognition refers to the capability for a device to recognize targets or other objects based on the microwave signals scattered from the targets and obtained from radar detectors, which has been widely used in both military and civil applications, such as enemy warning radar systems, ballistic missile defense systems, and civil air traffic control systems [1].

Target recognition can be categorized into two different classes, namely, cooperative and noncooperative target recognition, depending on whether communication links are established between the radar detectors and the targets to be recognized [1]. Cooperative target recognition was introduced during World War II with the invention of identification friend or foe (IFF) systems, which are friend or foe traffic control recognition devices and systems designed to prevent military friendly fire incidents, detect potential adversary incursions, support operational decision-making, and reduce casualties in the air, on land, and at sea. A typical IFF system includes an interrogator and a transponder. It uses the transponder to listen for the interrogating signal and then sends a response that identifies the broadcaster, while a noncooperative identification system can identify unknown targets with no need to establish communication link with the target. These systems are realized by comparing the observed scattered data with a database of potential targets to determine the closest match.

During the past decade, metasurfaces, the 2-D engineered surfaces exhibiting unique features not found in nature, have been of significant interest in a wide range of research areas because of their dramatic benefits of low profile, low cost, and the strong capability of manipulating electromagnetic waves [2], [3], [4]. Many metasurface-based applications have been studied, including wavefront reshaping [5], near-field focusing [6], polarization conversion [7], [8], [9], power absorption [10], [11], cloaking [12], [13], energy harvesting [14], and holography [15], [16], to name a few.

More recently, time-modulated metasurfaces have been proposed to further enhance the wave manipulation capacity of metasurfaces [17], [18], [19], [20], [21]. By revoking the fundamental constraints of linear time-invariant systems and adding a new manipulating freedom of time, time-modulated metasurfaces open a new avenue for the development of metasurface technologies, and a variety of applications have been reported, such as electromagnetic camouflaging [22], [23], [24], microwave imaging [25], magnetless nonreciprocity [26], [27], [28], [29], [30], [31], spectrum conversion [32], [33], direction-of-arrival (DoA) estimation [34], [35], [36], [37], sideband free antennas [38], analog signal processing [39], and simplified wireless communication and radar systems [40], [41], [42], [43].

In this article, pseudorandom noise (PN) sequence time-modulated reflective metasurfaces are proposed for the application of target recognition, which provides a low-cost, low-complexity, simple solution for recognizing targets. PN sequences are sequences similar to random sequences, which generally have properties similar to random sequences, such as strong autocorrelation and weak cross correlation [44]. By covering the target to be recognized with a time-modulated metasurface that is modulated by a PN time

Manuscript received 5 April 2023; accepted 29 April 2023. Date of publication 24 May 2023; date of current version 7 August 2023. This work was supported by the Shanghai Pujiang Program under Grant 22PJD072. *(Corresponding authors: Mei Song Tong; Lei Zhao.)*

Xiaoyi Wang and Mei Song Tong are with the College of Electronic and Information Engineering, Tongji University, Shanghai 201804, China (e-mail: xiaoyiwang@tongji.edu.cn; mstong@tongji.edu.cn).

Lei Zhao is with the School of Information and Control Engineering, China University of Mining and Technology, Xuzhou 221116, China (e-mail: leizhao@cumt.edu.cn).

Color versions of one or more figures in this article are available at https://doi.org/10.1109/TMTT.2023.3276050.

Digital Object Identifier 10.1109/TMTT.2023.3276050

0018-9480 © 2023 IEEE. Personal use is permitted, but republication/redistribution requires IEEE permission.
See https://www.ieee.org/publications/rights/index.html for more information.

Authorized licensed use limited to: CHINA UNIVERSITY OF MINING AND TECHNOLOGY. Downloaded on November 14,2023 at 23:46:33 UTC from IEEE Xplore. Restrictions apply.

sequence, the metasurface will scatter the interrogating harmonic wave into a binary PN phase-modulated wave. Therefore, the radar detector with the foreknowledge of the modulating PN sequence may recognize the target by applying the properties of strong autocorrelation and weak cross correlation of PN sequences and performing cross correlation between the modulating PN sequence and the picked-up signal after downshifting its frequency without actually decoding and reading the scattered information. The proposed time-modulated reflective metasurface-based target recognition may be seen as noncooperative target recognition, since the metasurfaces do not read the incident wave and radiate any signal by themselves; therefore, no real communication link between the detector and the metasurface is established. However, it does have the key features of cooperative target recognition, since the scattered wave carries the metasurface modulating information, which is unique and can be used to recognize the object covered by the metasurface. Compared with conventional passive tag-based radio frequency identification (RFID) technologies, which are usually applied in short-range applications, the proposed time-modulated reflective metasurface-based target recognition is nearly passive and can realize target recognition in a much longer range due to the large number of elements on the metasurfaces. In addition, it can realize the target in more flexible ways by applying the strong capability of wave manipulation of metasurfaces; for instance, the transmitter and receiver can be placed at different locations, by designing a metasurface with beam steering function; the scattered signals can be directed to multiple receivers located at different positions by designing a beam splitting metasurface. The proposed time-modulated reflective metasurface may find applications in long-range target recognition applications, such as unmanned aerial vehicles and self-driving cars.

The rest of this article is organized as follows. Section II describes the general concept and the operating principle of the proposed target recognition based on PN sequence time-modulated metasurfaces. Then, Section III provides the 1-bit metasurface unit cell design for PN sequence time modulation with full-wave simulation. Next, Section IV demonstrates the proposed PN time-modulated metasurface-based target recognition in two different scenarios by experiment. Finally, Section V concludes this article.

II. General Concept and Operating Principle

A. Concept

Fig. 1 illustrates the general concept of the proposed target recognition based on PN sequence time-modulated reflective metasurfaces, where the detector may recognize whether particular targets are present or not and distinguish specified target from a group of targets. A detector that contains a transmitter and a receiver sends a harmonic interrogating wave $\psi_t(t) = e^{-j\omega_0 t}$ toward the targets. Each of the present targets to be recognized is covered by a metasurface that is time modulated by a different PN sequence driven by a field-programmable gate array (FPGA) platform, which is unique information of the metasurface and is the foreknowledge for the detector. The incident wave impinges on the metasurfaces and interacts with the different time modulations on different metasurfaces. The waves scattered by all the metasurfaces are picked up by the receiver of the detector and analyzed in the postprocessing stage. After postprocessing, the detector may identify particular targets by applying the time-modulation foreknowledge.

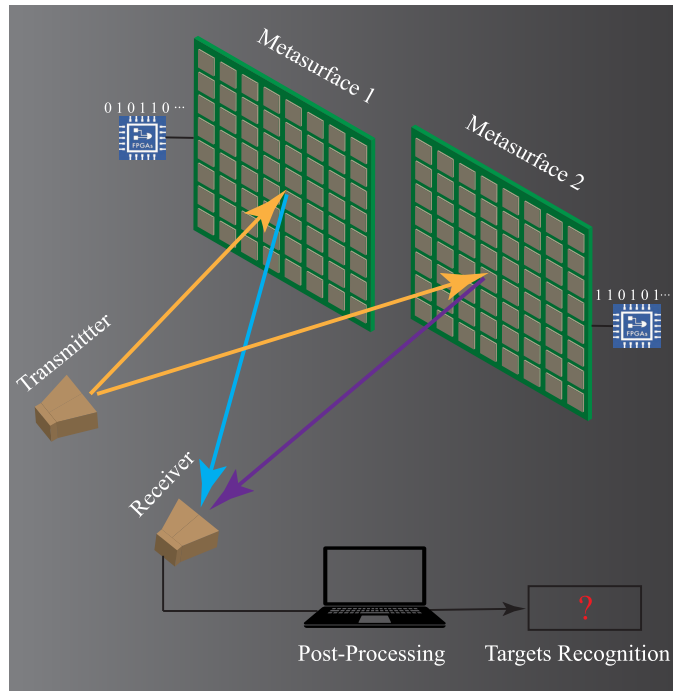

Fig. 1. Conceptual illustration of the proposed target recognition based on pseudorandom (PN) sequence time-modulated reflective metasurfaces, where the detector may recognize whether particular targets are present or not and distinguish specified target from a group of targets.

B. Scattered Wave of Time-Modulated Reflective Metasurfaces

Consider a slowly time-modulated reflective metasurface that operates at the angular frequency ω_0 and is time modulated by a time-varying signal $m(t)$, leading to a time-varying reflective coefficient of $\Gamma(t, \omega_0)$. When a harmonic wave $\psi_t(t) = e^{-j\omega_0 t}$ impinges on the metasurface, the reflective wave $\psi_r(t)$ scattered by the metasurface is then written as follows:

$$\psi_r(t) = \Gamma(t, \omega_0)\psi_t(t) = \Gamma(t, \omega_0)e^{-j\omega_0 t}. \tag{1}$$

Equation (1) shows that the reflective wave $\psi_r(t)$ can be seen as a signal with the envelope of $\Gamma(t, \omega_0)$ is frequency upshifted to the carrier frequency of ω_0. Noting that the slow modulation should be satisfied here to safely decouple the dispersion and time-varying effects of the time-varying reflective coefficient $\Gamma(t, \omega_0)$, which requires that the time-modulation rate f_m should be much lower than the operating frequency $f_0 = \omega_0/(2\pi)$ [17], [21], [23]. Under this condition, the parameters used to describe time-invariant systems, such as scattering parameters, are still quasi-valid in a slowly time-varying system.

C. PN Sequence Time-Modulated Reflective Metasurfaces

In this work, PN sequence, specifically, maximum length sequence, is chosen as the modulating signal $m(t)$, which is

Authorized licensed use limited to: CHINA UNIVERSITY OF MINING AND TECHNOLOGY. Downloaded on November 14,2023 at 23:46:33 UTC from IEEE Xplore. Restrictions apply.

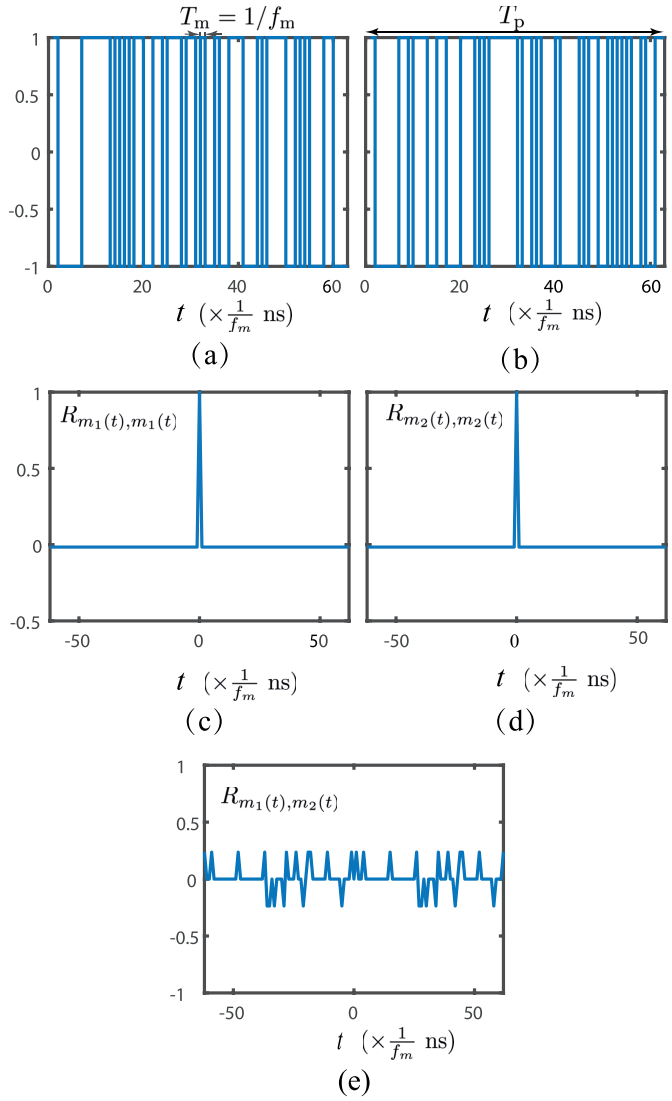

Fig. 2. Examples of PN sequence properties. (a) Waveform of PN sequence, $m_1(t)$. (b) Waveform of PN sequence, $m_2(t)$. (c) Autocorrelation of PN sequence, $m_1(t)$. (d) Autocorrelation of PN sequence, $m_2(t)$. (e) Cross correlation between PN sequences, $m_1(t)$ and $m_2(t)$.

a binary periodic sequence generated using maximal linear-feedback shift registers, exhibiting the features of balanced $+1$ and -1 numbers, a strong autocorrelation property (close to the Dirac delta function function), and week cross correlation between different sequences. These PN sequences may be represented as coefficients of irreducible polynomials in a polynomial ring [44]. Fig. 2 shows the examples of the properties of PN sequences. Fig. 2(a) and (b) shows the waveforms of a period of two different PN sequences, $m_1(t)$ and $m_2(t)$. The two PN sequences have the same periodic length $L = 63$, but are generated by different coefficients of irreducible polynomials [6, 1] and [6, 5, 2, 1], respectively. Fig. 2(c) and (d) plots the autocorrelation results of the two PN sequences shown in Fig. 2(a) and (b), whose results may be expressed as follows [44]:

$$R_{m(t),m(t)}(t) = \frac{1}{T_p}\int_0^{T_p} m(\tau)m(\tau+t)d\tau = \begin{cases} 1, & t = 0 \\ -\dfrac{1}{L}, & t \neq 0 \end{cases} \tag{2}$$

which approximates the Dirac delta function, $\delta(t)$, when $L \gg 1$. Fig. 2(e) plots the cross-correlation result between the two PN sequences, $m_1(t)$ and $m_2(t)$. It shows that the peak value of the cross-correlation results is much smaller compared with the peak value of the autocorrelation of the two PN sequences shown in Fig. 2(c) and (d). By applying these properties of strong autocorrelation and weak cross correlation of the PN sequences, target recognition may be achieved by using PN sequence time-modulated metasurfaces.

Considering a scenario that there are N different metasurfaces with each of them are time modulated by a different binary PN sequence $m_n(t)$, where $n = 1, 2, \ldots, N$, and assuming the time-varying reflective coefficient of the nth metasurface at the angular frequency ω_0, $\Gamma_n(t, \omega_0)$, is equivalent to the modulating sequence $m_n(t)$; namely, when the binary modulating sequence is $+1$, the reflective coefficient of the metasurface is $+1$; otherwise, the reflective coefficient of the metasurface is -1. The total reflective wave scattered by all the N time-modulated metasurfaces $\psi_{r,\text{total}}(t)$ is then expressed as follows:

$$\psi_{r,\text{total}}(t) = \sum_{n=1}^{n=N} \Gamma_n(t-\tau_n, \omega_0)e^{-j\omega_0 t} \tag{3}$$

where τ_n is the time delay between the incident wave arrives at the first and nth metasurfaces.

In the postprocessing stage, the picked-up signal is first downshifted to zero frequency, namely,

$$\psi_{r,\text{ds}}(t) = \sum_{n=1}^{n=N} \Gamma_n(t-\tau_n, \omega_0). \tag{4}$$

Then, cross correlation between the kth metasurface modulating PN sequence $m_k(t)$ and the downshifted signal $\psi_{r,\text{ds}}(t)$ in a period is performed, which is

$$\begin{aligned} R_k(t) &= \frac{1}{T_p}\int_0^{T_p} m_k(\tau)\psi_{r,\text{ds}}(\tau+t)d\tau \\ &= \frac{1}{T_p}\sum_{n=1}^{n=N}\int_0^{T_p} m_k(\tau)\Gamma_n(\tau+t-\tau_n, \omega_0)d\tau \\ &= \frac{1}{T_p}\sum_{n=1}^{n=N}\int_0^{T_p} m_k(\tau)m_n(\tau+t-\tau_n, \omega_0)d\tau \\ &= \frac{1}{T_p}\int_0^{T_p} m_k(\tau)m_k(\tau+t-\tau_k, \omega_0)d\tau \\ &\quad + \sum_{n=1}^{n=N, n\neq k}\frac{1}{T_p}\int_0^{T_p} m_k(\tau)m_n(\tau+t-\tau_n, \omega_0)d\tau \\ &\approx \delta(t-\tau_k) \\ &\quad + \sum_{n=1}^{n=N, n\neq k}\frac{1}{T_p}\int_0^{T_p} m_k(\tau)m_n(\tau+t-\tau_n, \omega_0)d\tau. \end{aligned} \tag{5}$$

Due to the weak cross-correlation property of PN sequence, the peak value of the second term in the last equivalent of (5) is much smaller than the peak value of the Dirac delta function in the first term, and the maximum value of $R_k(t)$ mainly depends on the maximum of the Dirac delta function. Therefore, by giving an appropriate threshold to detect the maximum value of $R_k(t)$, specifically, if the maximum value of $R_k(t)$ is larger than the threshold, the metasurface that is modulated by the PN sequence $m_k(t)$ is recognized to be presented in the metasurfaces. However, if the maximum

Authorized licensed use limited to: CHINA UNIVERSITY OF MINING AND TECHNOLOGY. Downloaded on November 14,2023 at 23:46:33 UTC from IEEE Xplore. Restrictions apply.

value of $R_k(t)$ is smaller than the threshold, it means the metasurface that is modulated by the PN sequence $m_k(t)$ is not present. Furthermore, the peak value of the Dirac delta function $\delta(t-\tau_k)$ in the last equivalent of (5) is time-shifted to τ_k due to the fact the metasurfaces may not be present at the same location. Therefore, by measuring the different peak values of the correlation results between $\psi_{r,\mathrm{ds}}(t)$ and different PN sequences, for instance, τ_p and τ_q, which represent the correlation results between $\psi_{r,\mathrm{ds}}(t)$ and $m_p(t)$ and $m_q(t)$, respectively, the distance between the pth and qth metasurfaces is then calculated by

$$d_{pq} = c_0(\tau_p - \tau_q) \tag{6}$$

where c_0 is the velocity of light in free space.

D. Noise Effect for Target Recognition

The good autocorrelation and cross-correlation properties of PN sequences play a crucial role in the applications of time-modulated metasurface for target recognition. However, the noise from both surrounding environment and the detector devices may reduce the signal-to-noise ratio (SNR) of the signal picked up by the detector and then further breaks the autocorrelation and cross-correlation properties of PN sequences. Fig. 3 plots the correlation performance of PN sequences under different SNRs, where Fig. 3(a) plots the autocorrelation performance and Fig. 3(b) plots the cross-correlation performance. It can be seen that when the SNR of the received signal is lower than 0 dB, the performance deteriorates quickly, and when the SNR is lower than −10 dB, the targets cannot be recognized anymore. However, the SNR of received signal may be greatly improved by using the techniques, such as improving the power of the incident wave, using metasurfaces with larger size, using a low noise amplifier (LNA), and performing matching filtering in the receiver.

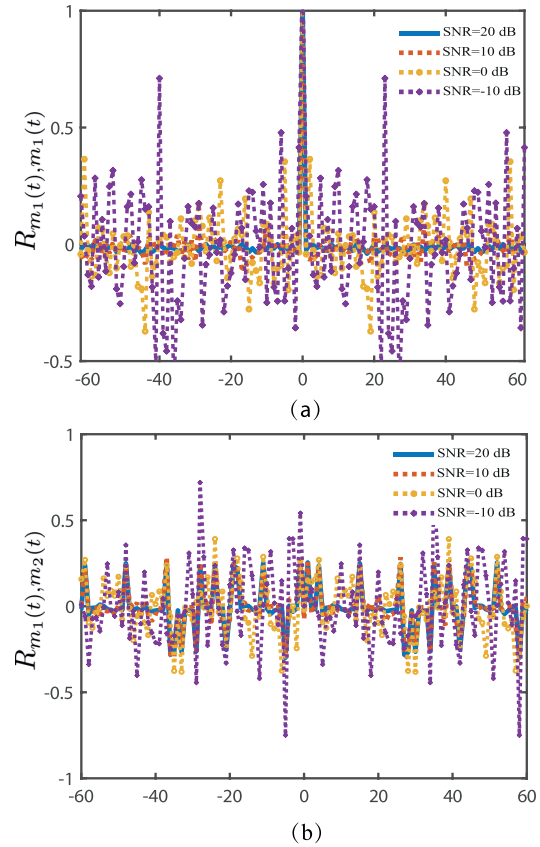

Fig. 3. Correlation performance of PN sequences under different SNRs. (a) Autocorrelation performance. (b) Cross-correlation performance.

TABLE I
METASURFACE UNIT CELL DESIGN PARAMETERS (UNIT: mm)

h_1	1.575	l_1	9
h_2	0.508	l_2	7
w_x	40	w_p	62.5
w_y	47	w_2	1.6

III. METASURFACE UNIT CELL DESIGN

A metasurface unit cell operating at 2.4 GHz is proposed and designed for the PN sequence time-modulated reflective metasurface. Fig. 4 provides the designed 1-bit tunable metasurface unit cell. Fig. 4(a) shows the side view of the metasurface unit cell, which is composed of three metal layers that are formed by two Rogers 5880 dielectric substrates whose dielectric constant is 2.9 and loss tangent is 0.002. The top and bottom layers of the metasurface unit cell are connected through metalized vias. A p-i-n diode is placed on the bottom layer of the metasurface unit cell with one of its side pins connected to the middle layer through a metalized via. Fig. 4(b) shows the top layer of the metasurface unit cell, which is a rectangular patch. Fig. 4(c) shows the middle layer of the metasurface unit cell. The middle layer is a ground layer with two circular slots to avoid the vias being shorted to the ground. Fig. 4(d) shows the bottom layer of the metasurface unit cell, which consists of two different parts. The key device of the left part of the bottom layer is a p-i-n diode with its right pin connected to the top-layer patch and the left pin shorted to the middle-layer ground. The right part of the bottom layer is a high impendence biasing line that is composed of a quarter wavelength transmission line and a pair of fan patches. The left-hand side of the biasing line is connected to the centering point of the top-layer patch to further avoid microwave wave energy leakage due to the fact that when the top-layer patch is resonant, standing wave is present in the top-layer patch, where the centering point is the null of the standing wave.

The mechanism of the proposed 1-bit tunable metasurface unit cell may be understood as follows. An x-polarized incident wave impinges on the metasurface; the wave is picked up by the top-layer patch and arrives at the right pin of the p-i-n diode on the bottom layer through the metalized via. If the p-i-n diode is off, the wave is reflected to the top-layer patch by the diode with the reflective coefficient −1 and is reradiated to the free space. If the p-i-n diode is on, the wave arrives at the right pin of the p-i-n diode on the bottom layer that passes the diode and is then reflected by the middle-layer ground with the reflective coefficient +1. Therefore, the reflective coefficients of the metasurface when the diode is off and on are out of phase. The equivalent circuits of the p-i-n diode in ON and OFF states used in this work are shown in Fig. 5, and the detailed design parameters of the metasurface unit cell are listed in Table I.

Authorized licensed use limited to: CHINA UNIVERSITY OF MINING AND TECHNOLOGY. Downloaded on November 14,2023 at 23:46:33 UTC from IEEE Xplore. Restrictions apply.

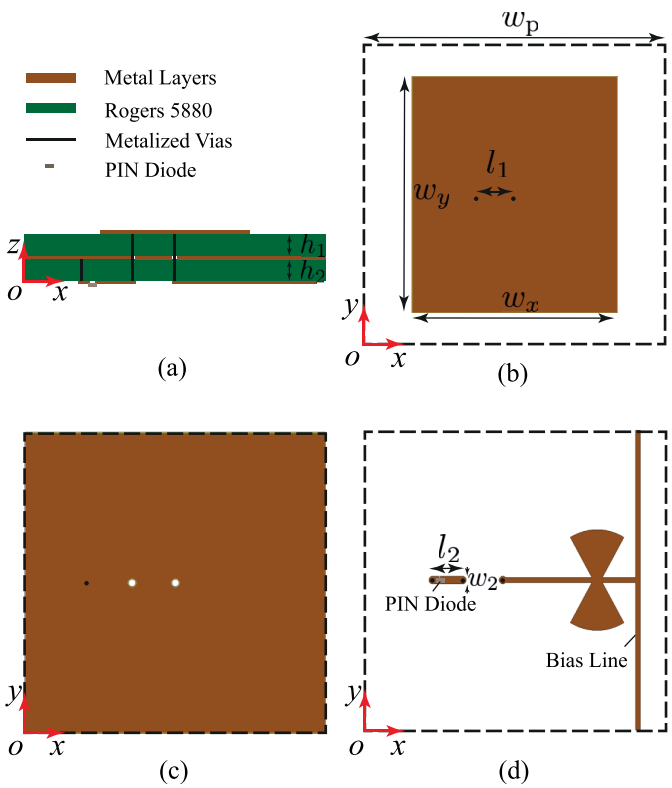

Fig. 4. 1-bit tunable metasurface unit cell. (a) Side view. (b) Top layer. (c) Middle layer. (d) Bottom layer.

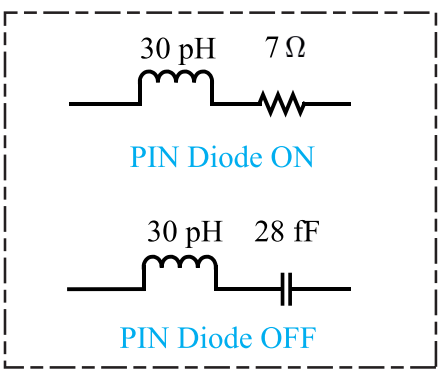

Fig. 5. Equivalent circuits of the p-i-n diode ON and OFF states.

Fig. 6 plots the full-wave simulation results of the designed metasurface unit cell when the p-i-n diode is at ON and OFF states. Fig. 6(a) plots the amplitude of the reflective coefficient of the proposed metasurface. In both cases, the metasurface reflects most of the incident energy at the operating frequency of 2.4 GHz, and a small part of the incident energy is dissipated due to the loss of the substrate and the p-i-n diodes. Fig. 6(b) plots the phase of the reflective coefficient of the proposed metasurface. Out-of-phase responses at 2.4 GHz are realized when the p-i-n diode is at ON and OFF states, respectively.

IV. Experimental Demonstration

An experiment is performed to demonstrate the proposed target recognition based on the designed PN sequence time-modulated reflective metasurfaces. The time-modulating rate f_m is set as 10 MHz in the following experiment, and two different scenarios are considered. In the first scenario,

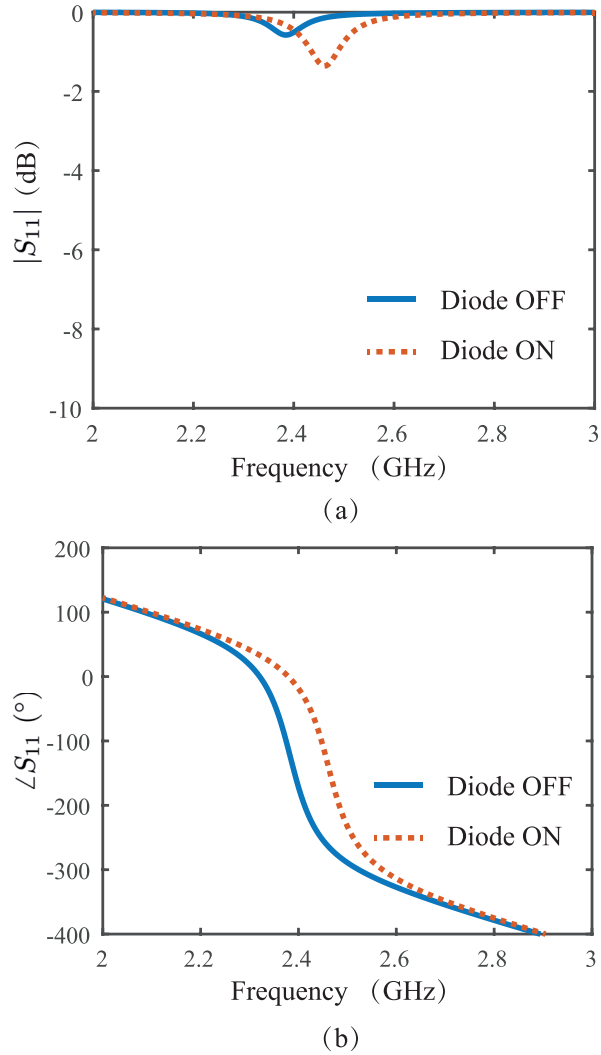

Fig. 6. Full-wave simulation results of the designed metasurface unit cell where the p-i-n diode is at ON and OFF states. (a) Amplitudes of the reflective coefficients. (b) Phases of the reflective coefficients.

only one piece of PN time-modulated reflective metasurface is present. The time-modulated reflective metasurface is modulated by $m_1(t)$ [Fig. 2(a)] with the coefficients of irreducible polynomials [6, 1]. In the postprocessing stage, the cross correlation between the downshifted received signal $\psi_{r,\mathrm{ds}}(t)$ and $m_1(t)$ is performed to recognize the metasurface. In the second scenario, two pieces of PN time-modulated reflective metasurface are present. The two time-modulated reflective metasurfaces are modulated by $m_1(t)$ [Fig. 2(a)] and $m_2(t)$ [Fig. 2(b)], with the coefficients of irreducible polynomials [6, 1] and [6, 5, 2, 1], respectively. There is another piece of PN time-modulated metasurface whose modulating sequence is $m_3(t)$ with the coefficients of irreducible polynomials [6, 3, 2, 1] not present in the scenario. In order to distinguish the two present metasurfaces, the two metasurfaces should be placed at different positions ideally. However, due to the limitation of the laboratory space, instead of physically placing the two metasurfaces in different locations, a modulating time delay $\Delta t = 20$ ns between the two modulating sequences $m_1(t)$ and $m_2(t)$ is applied; namely, $m_1(t)$ and $m_2(t - \Delta t)$ are used to modulate the two metasurfaces located at the same position to simulate the

Authorized licensed use limited to: CHINA UNIVERSITY OF MINING AND TECHNOLOGY. Downloaded on November 14,2023 at 23:46:33 UTC from IEEE Xplore. Restrictions apply.

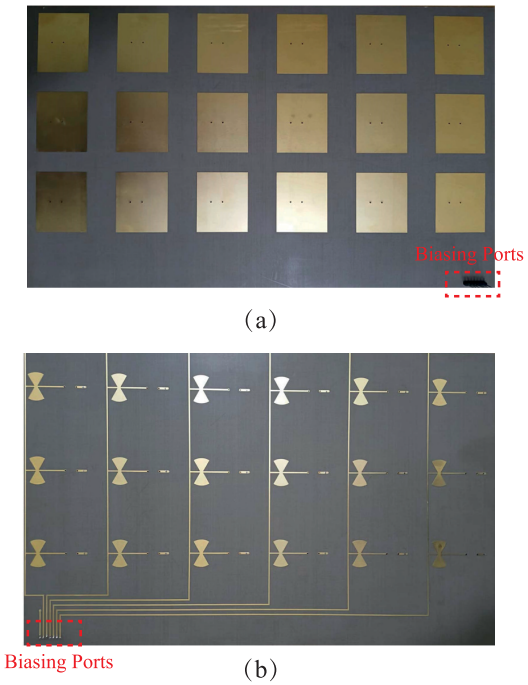

Fig. 7. Photographs of fabricated metasurface prototype. (a) Top view. (b) Bottom view.

case that the two metasurfaces are synchronized with the first metasurface that is modulated by $m_1(t)$ is $d = c_0\Delta t = 6$ m closer to the detector than the second metasurface that is modulated by $m_2(t)$. In the postprocessing stage, the cross correlations among the downshifted received signals $\psi_{r,\mathrm{ds}}(t)$ and $m_1(t)$, $m_2(t)$, and $m_3(t)$ are performed to recognize the metasurfaces, respectively.

Fig. 7 shows the prototype of a piece of fabricated metasurface with 3×6 elements, where Fig. 7(a) shows the top view and Fig. 7(b) shows the bottom view of the metasurface prototype, respectively. In the designed metasurface, the elements of each column of the metasurface are connected in series and controlled by a time-varying PN biasing voltage sequence. All the columns are biased by the same PN biasing voltage sequence; therefore, all the elements on the metasurface can be switched on and off simultaneously. Fig. 8 illustrates the experimental setup. Fig. 8(a) shows the experimental setup diagram. The metasurfaces are placed in front of a piece of absorbing material. The time modulation is realized using an FPGA platform. The harmonic interrogating signal with the frequency $f_0 = 2.4$ GHz is generated by a signal generator and radiated by a transmitting horn antenna toward the metasurfaces. The wave scattered by the metasurfaces is first picked by a receiving horn antenna, then processed by a bandpass filter, a frequency downshifting mixer with local oscillator (LO) frequency f_0, and a 0–50-MHz low-pass filter, and finally displayed and stored by an oscilloscope. Fig. 8(b) shows the photograph of the experimental setup.

Fig. 9 plots the normalized waveform in one period picked up by the oscilloscope $\psi_{r,\mathrm{ds}}(t)$ for the first scenario where only one time-modulated metasurface is present. The waveform keeps well the main envelope of the modulating PN sequence $m_1(t)$ shown in Fig. 2(a). Fig. 10 plots the normalized cross-correlation result between the modulating PN sequence $m_1(t)$ and the measured waveform picked up by the oscilloscope

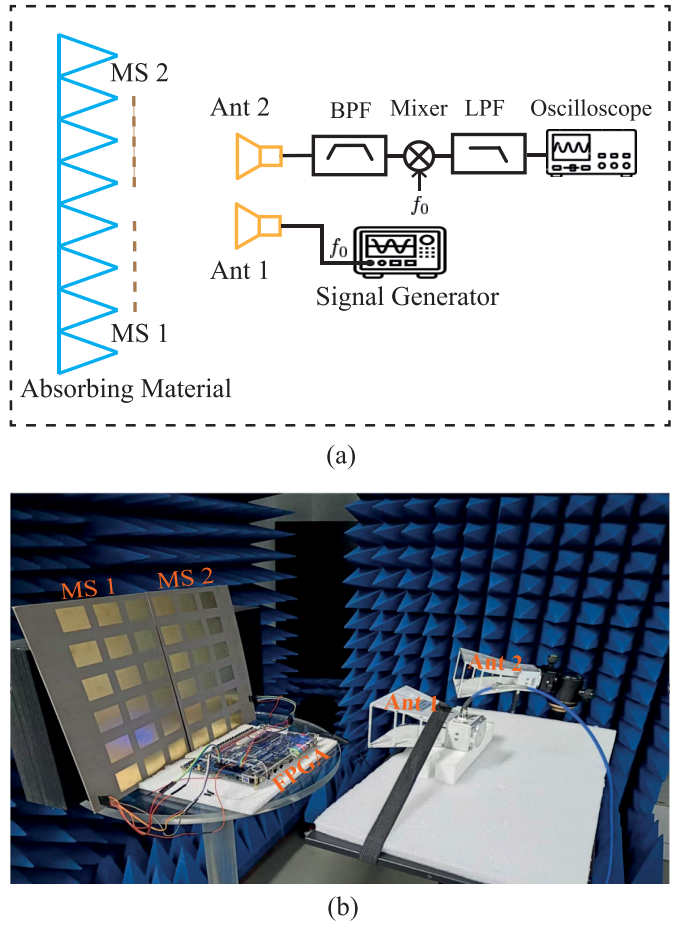

Fig. 8. Experimental setup. (a) Experimental setup diagram. (b) Photograph of the setup with the fabricated metasurface prototype.

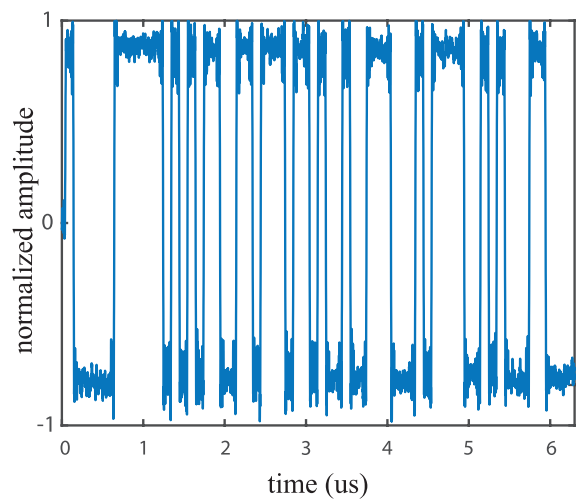

Fig. 9. Normalized waveform in one period picked up by the oscilloscope for the first scenario where only one time-modulated reflective metasurface is present.

$\psi_{r,\mathrm{ds}}(t)$ in Fig. 9. The cross-correlation result approximates a Dirac function $\delta(t)$, which demonstrates that by providing an appropriate threshold, the peak of the cross-correlation result can be detected larger than the threshold; therefore, the time-modulated metasurface whose modulating sequence is $m_1(t)$ is recognized. If the target that is covered by the metasurface is moving, Doppler shift will be introduced in the reflective wave, which will break the correlation property between the

Authorized licensed use limited to: CHINA UNIVERSITY OF MINING AND TECHNOLOGY. Downloaded on November 14,2023 at 23:46:33 UTC from IEEE Xplore. Restrictions apply.

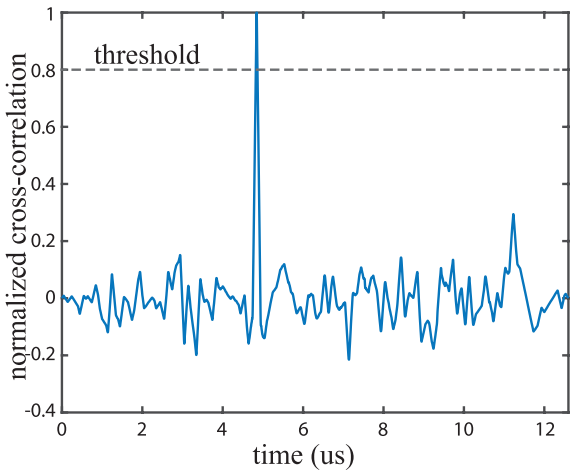

Fig. 10. Normalized cross-correlation result between the modulating PN sequence $m_1(t)$ and the measured waveform picked up by the oscilloscope in Fig. 9.

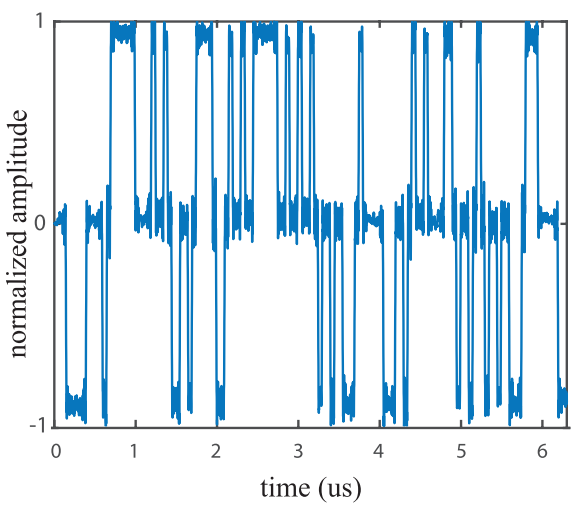

Fig. 11. Normalized waveform in one period picked up by the oscilloscope for the second scenario where two different time-modulated reflective metasurfaces are present.

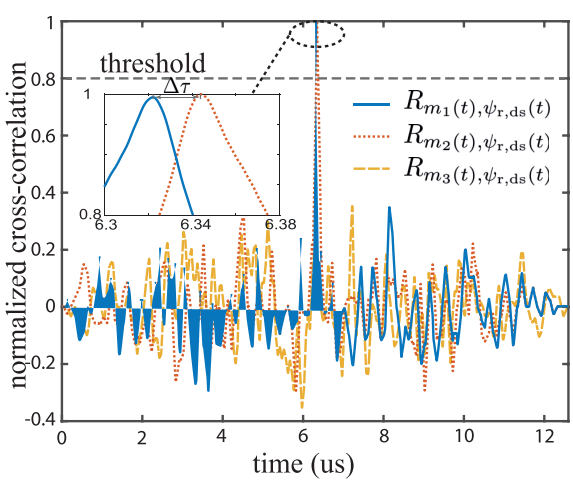

Fig. 12. Normalized cross-correlation results between the measured waveform picked up by the oscilloscope in Fig. 11 and the modulating PN sequences, $m_1(t)$, $m_2(t)$, and $m_3(t)$, respectively.

received signal and the modulated PN sequence. In this case, carrier frequency offset estimation and compensation should be performed in the receiver to remove the Doppler effect,

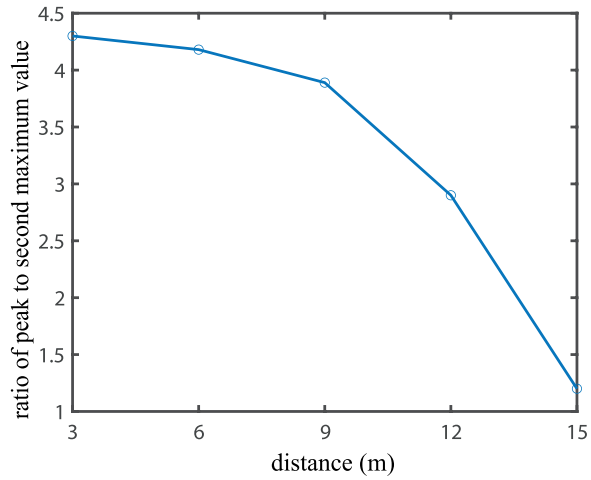

Fig. 13. Ratio of the peak value to the second maximum value in the correlation results, as the distance between the metasurface and the detector varies, where the power of the harmonic incident wave is −15 dBm.

which are widely used in current wireless communication receiver design [45].

Fig. 11 plots the normalized waveform in one period picked up by the oscilloscope $\psi_{r,\mathrm{ds}}(t)$ for the second scenario where two time-modulated reflective metasurfaces are present, whose modulating sequences are $m_1(t)$ and $m_2(t)$, respectively. Fig. 12 plots the normalized cross-correlation results between the measured waveform picked up by the oscilloscope $\psi_{r,\mathrm{ds}}(t)$ in Fig. 11, and the modulating PN sequences, $m_1(t)$, $m_2(t)$, and $m_3(t)$, respectively. It shows that both of the metasurfaces that are modulated by $m_1(t)$ and $m_2(t)$ are recognized being present by detecting their peaks of the cross-correlation results larger than the threshold, and the metasurface that is modulated by $m_3(t)$ is not present, since no peak is detected larger than the threshold. Meanwhile, the time delay among $R_{m_1(t)}$, $\psi_{r,\mathrm{ds}}(t)$, and $R_{m_1(t)}\psi_{r,\mathrm{ds}}(t)$ is measured, which is $\Delta\tau = \tau_2 - \tau_1 = 20.8$ ns, showing that the first metasurface that is modulated by $m_1(t)$ is $\Delta d_{\mathrm{meas.}} = c_0\Delta\tau = 6.24$ m closer to the detector than the second metasurface that is modulated by $m_2(t)$. The 0.24-m deviation is caused by the distortion of the signal picked up by the oscilloscope, which may be introduced by several factors, such as noise from the environment and the receiving devices, the spectrum loss from filters, the frequency offset in the mixer, and the nonideal responses of the metasurfaces. Noting that the proposed time-varying metasurface-based target recognition only works for the scenario where the distance between targets is far smaller than the distance from the targets to the detector. Otherwise, the power reflected by the far targets may be too weak, and the peak of their correlation will be masked by the cross correlation of targets close to the detector.

Fig. 13 plots the ratio of the peak value to the second maximum value in the correlation results, as the distance between the metasurface and the detector increases. Due to the limited space in our laboratory, a harmonic wave with relatively small power, −15 dBm, is generated by the signal generator for the transmitting antenna to illuminate the metasurface. It can be seen from Fig. 13 that when the distance is smaller than 9 m, the ratio of the peak value to the second maximum value in the correlation results decreases slowly; while when the distance is larger than 9 m, the ratio decreases

Authorized licensed use limited to: CHINA UNIVERSITY OF MINING AND TECHNOLOGY. Downloaded on November 14,2023 at 23:46:33 UTC from IEEE Xplore. Restrictions apply.

quickly; when the distance is 15 m, the ratio is close to 1, which means the targets cannot be recognized anymore. This is because as the distance increases, the power picked up by the detector decreases, leading to a low SNR. This detecting distance can be largely enhanced by improving the SNR of the received signal using the techniques discussed in Section II-D.

V. Conclusion

In conclusion, we propose a low-cost, low-complexity, simple solution for target recognition based on PN sequence time-modulated reflective metasurfaces. By covering the target to be recognized with a PN sequence time-modulated reflective metasurface, the metasurface may scatter the interrogating harmonic wave from the detector into a unique PN-modulated wave. By applying the foreknowledge of the modulating PN sequence and performing cross correlation between the modulating PN sequence and the picked-up signal after downshifting to zero frequency, the detector can perfectly recognize whether specified metasurfaces are present or not, distinguish different targets located at different locations, and estimate the distances between different targets. A tunable metasurface unit cell with out-of-phase states is studied, and the overall metasurface-based target recognition is demonstrated by experiment in different scenarios. The proposed noncooperative metasurface-based target recognition exhibits the features of cooperative target recognition, although no real communication link between the detector and the metasurface is established, which may find potential applications in both military and civil long-range target recognition applications for low-cost, high-efficient target recognition.

References

[1] P. Tait, *Introduction to Radar Target Recognition*. Edison, NJ, USA: IET, Futures Place, 2005.

[2] H.-T. Chen, A. J. Taylor, and N. Yu, "A review of metasurfaces: Physics and applications," *Rep. Prog. Phys.*, vol. 79, no. 7, Jun. 2016, Art. no. 076401.

[3] J. Hu, S. Bandyopadhyay, Y.-H. Liu, and L.-Y. Shao, "A review on metasurface: From principle to smart metadevices," *Frontiers Phys.*, vol. 8, Jan. 2021, Art. no. 586087.

[4] X. Jia, X. Wang, and Y. Vahabzadeh, "Fast computation of resonant metasurfaces in FDTD scheme using dispersive surface susceptibility model," *IEEE Trans. Antennas Propag.*, vol. 71, no. 1, pp. 713–722, Jan. 2023.

[5] P. Genevet and F. Capasso, "Breakthroughs in photonics 2013: Flat optics: Wavefronts control with Huygens' interfaces," *IEEE Photon. J.*, vol. 6, no. 2, pp. 1–4, Apr. 2014.

[6] X. Wang, M. S. Tong, and G.-M. Yang, "Multifocus multinull near-field transmitting focused metasurface," *IEEE Trans. Antennas Propag.*, vol. 71, no. 4, pp. 3172–3182, Apr. 2023.

[7] T. Zhang, H. Wang, C. Peng, Z. Chen, and X. Wang, "C-band linear polarization metasurface converter with arbitrary polarization rotation angle based on notched circular patches," *Crystals*, vol. 12, no. 11, p. 1646, Nov. 2022.

[8] X. Wang and G.-M. Yang, "Linear-polarization metasurface converter with an arbitrary polarization rotating angle," *Opt. Exp.*, vol. 29, no. 19, pp. 30579–30589, 2021.

[9] J. Li et al., "Dual-band polarization-insensitive orbital angular momentum beam generation based on 1-bit polarization-converting transmitting coding metasurface," *Int. J. RF Microw. Comput.-Aided Eng.*, vol. 32, no. 11, Nov. 2022, Art. no. e23397.

[10] T. Deng et al., "Ultra-thin and broadband surface wave meta-absorber," *Opt. Exp.*, vol. 29, no. 12, pp. 19193–19201, Jun. 2021.

[11] Y. Wen, W. Ma, J. Bailey, G. Matmon, X. Yu, and G. Aeppli, "Planar broadband and high absorption metamaterial using single nested resonator at terahertz frequencies," *Opt. Lett.*, vol. 39, no. 6, pp. 1589–1592, 2014.

[12] D. Ramaccia, D. L. Sounas, A. Alù, A. Toscano, and F. Bilotti, "Doppler cloak restores invisibility to objects in relativistic motion," *Phys. Rev. B, Condens. Matter*, vol. 95, no. 7, Feb. 2017, Art. no. 075113.

[13] R. Fleury, F. Monticone, and A. Alù, "Invisibility and cloaking: Origins, present, and future perspectives," *Phys. Rev. Appl.*, vol. 4, no. 3, Sep. 2015, Art. no. 037001.

[14] A. A. G. Amer, S. Z. Sapuan, N. Nasimuddin, A. Alphones, and N. B. Zinal, "A comprehensive review of metasurface structures suitable for RF energy harvesting," *IEEE Access*, vol. 8, pp. 76433–76452, 2020.

[15] L. Huang, S. Zhang, and T. Zentgraf, "Metasurface holography: From fundamentals to applications," *Nanophotonics*, vol. 7, no. 6, pp. 1169–1190, Jun. 2018.

[16] G. Zheng, H. Mühlenbernd, M. Kenney, G. Li, T. Zentgraf, and S. Zhang, "Metasurface holograms reaching 80% efficiency," *Nature Nanotechnol.*, vol. 10, no. 4, pp. 308–312, Feb. 2015.

[17] L. Zhang et al., "Space-time-coding digital metasurfaces," *Nature Commun.*, vol. 9, no. 1, p. 4334, Oct. 2018.

[18] Y. Saifullah, Y. He, A. Boag, G.-M. Yang, and F. Xu, "Recent progress in reconfigurable and intelligent metasurfaces: A comprehensive review of tuning mechanisms, hardware designs, and applications," *Adv. Sci.*, vol. 9, Nov. 2022, Art. no. 2203747.

[19] L. Zhang and T. J. Cui, "Space-time-coding digital metasurfaces: Principles and applications," *Research*, vol. 2021, Jan. 2021, Art. no. e9802673.

[20] S. Taravati and G. V. Eleftheriades, "Microwave space-time-modulated metasurfaces," *ACS Photon.*, vol. 9, no. 2, pp. 305–318, Jan. 2022.

[21] S. Taravati and G. V. Eleftheriades, "4D wave transformations enabled by space-time metasurfaces: Foundations and illustrative examples," *IEEE Antennas Propag. Mag.*, early access, Sep. 12, 2022, doi: 10.1109/MAP.2022.3201195.

[22] X. Wang and C. Caloz, "Spread-spectrum selective camouflaging based on time-modulated metasurface," *IEEE Trans. Antennas Propag.*, vol. 69, no. 1, pp. 286–295, Jan. 2021.

[23] X. Wang and C. Caloz, "Pseudorandom sequence (space–) time-modulated metasurfaces: Principles, operations, and applications," *IEEE Antennas Propag. Mag.*, vol. 64, no. 4, pp. 135–144, Aug. 2022.

[24] M. Liu, A. B. Kozyrev, and I. V. Shadrivov, "Time-varying metasurfaces for broadband spectral camouflage," *Phys. Rev. Appl.*, vol. 12, no. 5, Nov. 2019, Art. no. 054052.

[25] M. Phaneuf and P. Mojabi, "On the use of reconfigurable space-time metasurface enclosures for microwave imaging," *IEEE Antennas Wireless Propag. Lett.*, vol. 21, no. 11, pp. 2196–2200, Nov. 2022.

[26] X. Guo, Y. Ding, Y. Duan, and X. Ni, "Nonreciprocal metasurface with space–time phase modulation," *Light, Sci. Appl.*, vol. 8, no. 1, p. 123, Dec. 2019.

[27] S. Taravati and G. V. Eleftheriades, "Full-duplex nonreciprocal beam steering by time-modulated phase-gradient metasurfaces," *Phys. Rev. Appl.*, vol. 14, no. 1, Jul. 2020, Art. no. 014027.

[28] X. Wang, J. Han, S. Tian, D. Xia, L. Li, and T. J. Cui, "Amplification and manipulation of nonlinear electromagnetic waves and enhanced nonreciprocity using transmissive space-time-coding metasurface," *Adv. Sci.*, vol. 9, no. 11, Feb. 2022, Art. no. 2105960.

[29] L. Zhang et al., "Breaking reciprocity with space-time-coding digital metasurfaces," *Adv. Mater.*, vol. 31, no. 41, Aug. 2019, Art. no. 1904069.

[30] B. Liu, S.-W. Wong, and Y. Li, "Rotational Doppler effect by space-time-coding metasurfaces for nonreciprocal electromagnetic isolation," *Opt. Exp.*, vol. 29, no. 15, pp. 24500–24507, Jul. 2021.

[31] A. E. Cardin et al., "Surface-wave-assisted nonreciprocity in spatio-temporally modulated metasurfaces," *Nature Commun.*, vol. 11, no. 1, pp. 1–9, Mar. 2020.

[32] Z. Wu and A. Grbic, "Serrodyne frequency translation using time-modulated metasurfaces," *IEEE Trans. Antennas Propag.*, vol. 68, no. 3, pp. 1599–1606, Mar. 2020.

[33] D. Ramaccia, D. L. Sounas, A. Alù, A. Toscano, and F. Bilotti, "Phase-induced frequency conversion and Doppler effect with time-modulated metasurfaces," *IEEE Trans. Antennas Propag.*, vol. 68, no. 3, pp. 1607–1617, Mar. 2020.

Authorized licensed use limited to: CHINA UNIVERSITY OF MINING AND TECHNOLOGY. Downloaded on November 14,2023 at 23:46:33 UTC from IEEE Xplore. Restrictions apply.

[34] X. Q. Chen, L. Zhang, S. Liu, and T. J. Cui, "Artificial neural network for direction-of-arrival estimation and secure wireless communications via space-time-coding digital metasurfaces," *Adv. Opt. Mater.*, vol. 10, no. 23, Sep. 2022, Art. no. 2201900.

[35] J. Y. Dai et al., "Simultaneous in situ direction finding and field manipulation based on space-time-coding digital metasurface," *IEEE Trans. Antennas Propag.*, vol. 70, no. 6, pp. 4774–4783, Jun. 2022.

[36] X. Fang et al., "Accurate direction–of–arrival estimation method based on space–time modulated metasurface," *IEEE Trans. Antennas Propag.*, vol. 70, no. 11, pp. 10951–10964, Nov. 2022.

[37] X. Wang and C. Caloz, "Direction-of-arrival (DOA) estimation based on spacetime-modulated metasurface," in *Proc. IEEE Int. Symp. Antennas Propag. USNC-URSI Radio Sci. Meeting*, Jul. 2019, pp. 1613–1614.

[38] G.-B. Wu, J. Y. Dai, Q. Cheng, T. J. Cui, and C. H. Chan, "Sideband-free space–time-coding metasurface antennas," *Nature Electron.*, vol. 5, no. 11, pp. 808–819, Nov. 2022.

[39] H. Rajabalipanah, A. Abdolali, S. Iqbal, L. Zhang, and T. J. Cui, "Analog signal processing through space-time digital metasurfaces," *Nanophotonics*, vol. 10, no. 6, pp. 1753–1764, Mar. 2021.

[40] J. Y. Dai et al., "Metasurfaces: Wireless communications through a simplified architecture based on time-domain digital coding metasurface (Adv. Mater. Technol. 7/2019)," *Adv. Mater. Technol.*, vol. 4, no. 7, Jul. 2019, Art. no. 1970037.

[41] X. Wang and G.-M. Yang, "Time-coding spread-spectrum reconfigurable intelligent surface for secure wireless communication: Theory and experiment," *Opt. Exp.*, vol. 29, no. 20, pp. 32031–32041, 2021.

[42] L. Zhang et al., "A wireless communication scheme based on space- and frequency-division multiplexing using digital metasurfaces," *Nature Electron.*, vol. 4, no. 3, pp. 218–227, Mar. 2021.

[43] X. Wan et al., "Joint radar and communication empowered by digital programmable metasurface," *Adv. Intell. Syst.*, vol. 4, no. 9, Jun. 2022, Art. no. 2200083.

[44] H.-J. Zepernick and A. Finger, *Pseudo Random Signal Processing: Theory and Application*. New York, NY, USA: Wiley, 2013.

[45] T.-D. Chiueh, P.-Y. Tsai, and I.-W. Lai, *Baseband Receiver Design for Wireless MIMO-OFDM Communications*. New York, NY, USA: Wiley, 2012.

Xiaoyi Wang (Member, IEEE) received the B.S. degree in electronic science and technology from the University of Electronic Science and Technology of China (UESTC), Chengdu, China, in 2011, the M.S. degree in communication and information system from Fudan University, Shanghai, China, in 2014, and the Ph.D. degree in electrical engineering from Polytechnique Montréal, Montréal, QC, Canada, in 2020.

He is currently a Research Professor with Tongji University, Shanghai. His research interests include all fields of theoretical, computational, and applied electromagnetics, with a strong emphasis on metamaterials and metasurfaces.

Dr. Wang was a recipient of the Student Paper Competition Award of the IEEE International Symposium on Antennas and Propagation (AP-S) in 2019 and the International Union of Radio Science (URSI) Young Scientist Award in 2020.

Mei Song Tong (Senior Member, IEEE) received the B.S. and M.S. degrees from the Huazhong University of Science and Technology, Wuhan, China, and the Ph.D. degree from Arizona State University, Tempe, AZ, USA, all in electrical engineering.

He was an Adjunct Professor with the University of Illinois at Urbana-Champaign, Urbana, IL, USA, and an Honorary Professor with the University of Hong Kong, Hong Kong, China. He is currently a Distinguished/Permanent Professor, the Head of the Department of Electronic Science and Technology, and the Vice Dean of the College of Microelectronics, Tongji University, Shanghai, China. He has authored or coauthored more than 500 papers in refereed journals and conference proceedings and coauthored six books or book chapters. His research interests include electromagnetic field theory, antenna theory and technique, modeling and simulation of RF/microwave circuits and devices, interconnect and packaging analysis, inverse electromagnetic scattering for imaging, and computational electromagnetics.

Prof. Tong is a Fellow of the Electromagnetics Academy, a Fellow of the Japan Society for the Promotion of Science (JSPS), and a Full Member (Commission B) of the United States National Committee (USNC)/International Union of Radio Science (URSI). He was a recipient of the Visiting Professorship Award from Kyoto University, Japan, in 2012, and from the University of Hong Kong, China, in 2013. He advised and coauthored 12 papers that received the Best Student Paper Award from different international conferences. He was also a recipient of the Travel Fellowship Award of USNC/URSI for the 31th General Assembly and Scientific Symposium (GASS) in 2014; the Advance Award of Science and Technology of Shanghai Municipal Government in 2015; the Fellowship Award of JSPS in 2016; the Innovation Award of Universities' Achievements of Ministry of Education of China in 2017; the Innovation Achievement Award of Industry-Academia-Research Collaboration of China in 2019; the Chapters Award of IEEE New Jersey Section, USA, in 2019; the "Jinqiao" Award of Technology Market Association of China in 2020; and the Baosteel Education Award of China in 2021. He has been the Chair of the Shanghai Chapter since 2014 and was the Chair of the Special Interest Group for Humanitarian Technology (SIGHT) Committee in 2018, respectively, in the IEEE Antennas and Propagation Society. He also frequently served as the session organizer/chair, technical program committee member/chair, and general chair for some prestigious international conferences. In 2018, he was selected as a Distinguished Lecturer (DL) of the IEEE Antennas and Propagation Society for 2019–2022. He has served as an Associate Editor or Guest Editor for some well-known international journals, including *IEEE Antennas and Propagation Magazine*, the IEEE TRANSACTIONS ON ANTENNAS AND PROPAGATION, the IEEE TRANSACTIONS ON COMPONENTS, PACKAGING AND MANUFACTURING TECHNOLOGY, the *International Journal of Numerical Modeling: Electronic Networks, Devices and Fields*, *Progress in Electromagnetics Research*, and the *Journal of Electromagnetic Waves and Applications*.

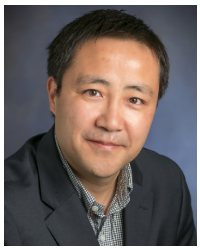

Lei Zhao (Senior Member, IEEE) received the B.S. degree in mathematics from Jiangsu Normal University, Xuzhou, China, in 1997, and the M.S. degree in computational mathematics and the Ph.D. degree in electromagnetic fields and microwave technology from Southeast University, Nanjing, China, in 2004 and 2007, respectively.

From August 2007 to August 2009, he worked with the Department of Electronic Engineering, The Chinese University of Hong Kong, Hong Kong, as a Research Associate. From September 2009 to December 2018, he worked with Jiangsu Normal University. From February 2011 to April 2011, he worked with the Department of Electrical and Computer Engineering, National University of Singapore, Singapore, as a Research Fellow. From September 2016 to September 2017, he worked with the Department of Electrical and Computer Engineering, University of Illinois at Urbana-Champaign, Champaign, IL, USA, as a Visiting Scholar. He joined the China University of Mining and Technology, Xuzhou, in 2019, where he is currently a Full Professor. He has authored or coauthored more than 100 refereed journal and conference papers. His current research interests include spoof surface plasmon polaritons theory and its applications, RF/Microwave antenna and filter design, computational electromagnetics, and electromagnetic radiation to human's body.

Dr. Zhao serves as an Associate Editor for IEEE ACCESS, an Associate Editor-in-Chief for *ACES Journal*, and a Reviewer for multiple journals and conferences, including the IEEE TRANSACTIONS ON MICROWAVE THEORY AND TECHNIQUES, the IEEE TRANSACTIONS ON ANTENNAS AND PROPAGATION, the IEEE ANTENNAS AND WIRELESS PROPAGATION LETTERS, *ACES Journal*, and other primary electromagnetics and microwave related journals.

Authorized licensed use limited to: CHINA UNIVERSITY OF MINING AND TECHNOLOGY. Downloaded on November 14,2023 at 23:46:33 UTC from IEEE Xplore. Restrictions apply.